

## Magnetic Bistability and Thermo-chromism in a Molecular Cu<sup>II</sup> Chain

Fatima Setifi,<sup>†,‡</sup> Samia Benmansour,<sup>†,§</sup> Mathieu Marchivie,<sup>†</sup> Gaëlle Dupouy,<sup>†</sup> Smail Triki,<sup>\*,†</sup> Jean Sala-Pala,<sup>†</sup> Jean-Yves Salaün,<sup>†</sup> Carlos J. Gómez-García,<sup>§</sup> Sébastien Pillet,<sup>||</sup> Claude Lecomte,<sup>||</sup> and Eliseo Ruiz<sup>⊥</sup>

UMR CNRS 6521, Université de Bretagne Occidentale, BP 809, 29285 Brest Cedex, France, Instituto de Ciencia Molecular, Parque Científico, Universidad de Valencia, 46980 Paterna, Spain, LCM3B, Nancy-Université, CNRS, Boulevard des Aiguillettes, BP 239, 54506 Nancy, France, and Departament de Química Inorgànica, Universitat de Barcelona, Diagonal 647, Barcelona 08028, Spain

Received December 1, 2008

An original magnetic bistability and a thermo-chromic transition are observed in a new Cu<sup>II</sup> molecular chain. Thermal structural studies reveal changes in the Cu<sup>II</sup> coordination sphere, driven by a more pronounced Jahn–Teller effect at low temperature. These distortions provoke a gradual color change. The structural study at 10 K shows a dimerization of the molecular chain, in agreement with the abrupt magnetic transition observed at 30 K.

Magnetic bistability, an interesting property resulting from a magnetic transition with hysteretic behavior, is one of the most searched properties in molecular materials nowadays because they may constitute the basis for the next generation of information storage devices.<sup>1–3</sup> Spin-crossover (SCO) complexes are one of the most representative examples of molecular bistable materials, which, in the particular case of the Fe<sup>II</sup> ion (d<sup>6</sup> configuration), present a paramagnetic–diamagnetic transition from the high-spin (*S* = 2) to the low-spin (*S* = 0) state.<sup>2</sup> Bistability is also encountered in some organic radical salts<sup>3</sup> and in a few inorganic compounds showing the so-called spin-Peierls (SP) or SP-like transitions.<sup>4</sup> From the structural point of view, most of the materials presenting a SP transition contain discrete molecular entities packed in columns via weak intermolecular interactions, such as M···S, S···S, or π–π contacts.<sup>3</sup> The

only exceptions are the two inorganic SP compounds CuGeO<sub>3</sub> and TiOCl, which display extended networks,<sup>3</sup> and the “possible SP” compound BBDTA·InCl<sub>4</sub>.<sup>3c</sup> In our ongoing work on metal-based polynitrile coordination polymers involving neutral bridging coligands,<sup>5</sup> we present here the synthesis, crystal structures at different temperatures, magnetic study, and theoretical calculations of [Cu(bpym)-(tcnoet)<sub>2</sub>]·H<sub>2</sub>O (**1**; tcnoet<sup>−</sup> = 1,1,3,3-tetracyano-2-ethoxypropene anion; bpym = 2,2′-bipyrimidine). This compound is the first covalently linked Cu<sup>II</sup> chain presenting magnetic bistability.

An aqueous solution (5 mL) of CuCl<sub>2</sub>·2H<sub>2</sub>O (27 mg, 0.16 mmol) was added to an ethanolic solution (5 mL) of bpym (25 mg, 0.16 mmol) with continuous stirring, leading to the immediate precipitation of a green powder. After the addition of an aqueous solution (6 mL) of K(tcnoet)<sup>6</sup> (72 mg, 0.32 mmol), the green precipitate was dissolved and the final green solution yielded by slow evaporation dark-red single crystals of **1**, which were removed by filtration and air-dried.<sup>7</sup>

At room temperature, **1** crystallizes in the monoclinic *I*2/a space group.<sup>8</sup> The bpym molecule acts as a bischelating ligand to generate a polymeric chain running along the *a* axis. The periodic motif is centrosymmetric with the inversion center in the middle of the central C4–C4 bond of the bpym (Figure 1). The Cu<sup>II</sup> ions lie on the crystallographic 2-fold axis (1/4, *y*, 0) and are octahedrally coordinated by two bpym ligands via the N1 and N2 atoms and by two (tcnoet)<sup>−</sup> polynitrile anions in a *cis* conformation (Figure 1).

\* To whom correspondence should be addressed. E-mail: triki@univ-brest.

<sup>†</sup> Université de Bretagne Occidentale.

<sup>‡</sup> On leave from the Département de Chimie, Faculté des Sciences, Université Ferhat Abbas, Sétif, Algeria.

<sup>§</sup> Universidad de Valencia.

<sup>||</sup> Nancy-Université.

<sup>⊥</sup> Universitat de Barcelona.

- (1) *Magnetism: Molecules to materials*; Drillon, M., Ed.; VCH: Weinheim, Germany, 2001.
- (2) (a) Bousseksou, A.; Molnár, G.; Real, J. A.; Tanaka, K. *Coord. Chem. Rev.* **2007**, *251*, 1822. (b) Gaspar, A. B.; Ksenofontov, V.; Serebryuk, M.; Güttlich, P. *Coord. Chem. Rev.* **2005**, *249*, 2661.
- (3) (a) Willett, R. D.; Gómez-García, C. J.; Ramakrishna, B. L.; Twamley, B. *Polyhedron* **2005**, *24*, 2232. (b) Fujita, W.; Awaga, K. *Science* **1999**, *286*, 261. (c) Fujita, W.; Awaga, K.; Kondo, R.; Kagoshima, S. *J. Am. Chem. Soc.* **2006**, *128*, 6016.

- (4) (a) Hase, M.; Terasaki, I.; Uchinokura, K. *Phys. Rev. Lett.* **1993**, *70*, 3651. (b) Ruiz, E.; Cano, J.; Alvarez, S.; Alemany, P.; Verdager, M. *Phys. Rev. B* **2000**, *61*, 54. (c) Seidel, A.; Marianetti, C. A.; Chou, F. C.; Ceder, G.; Lee, P. A. *Phys. Rev. B* **2003**, *67*, 0204051.
- (5) (a) Triki, S.; Thétiot, F.; Vandeveld, F.; Sala-Pala, J.; Gómez-García, C. J. *Inorg. Chem.* **2005**, *44*, 4086. (b) Thétiot, F.; Triki, S.; Sala-Pala, J.; Galan-Mascaros, J.-R.; Martínez-Agudo, J. M.; Dunbar, K. R. *Eur. J. Inorg. Chem.* **2004**, 3783.
- (6) Thétiot, F.; Triki, S.; Sala-Pala, J. *Polyhedron* **2003**, *22*, 1837.
- (7) Satisfactory elemental analysis data for C<sub>26</sub>H<sub>18</sub>CuN<sub>12</sub>O<sub>3</sub> for **1**. Found: C, 51.5; H, 2.9; N, 27.9; Cu, 10.1. Calcd: C, 51.2; H, 3.0; N, 27.5; Cu, 10.4. IR data (KBr, ν/cm<sup>−1</sup>) for **1**: 3424br, 3083w, 2999w, 2239s, 2208s, 1581s, 1559m, 1496s, 1469s, 1409s, 1375m, 1343m, 1221m, 1183m, 1143w, 1103w, 996m, 755m, 671m, 534m.

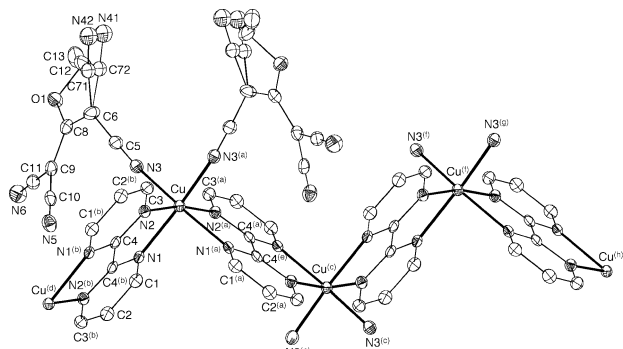


**Figure 1.** Perspective view of the regular chain of **1** (for the sake of clarity, only two polynitrile ligands are shown).

**Table 1.** Apparent Cu–N and Intrachain Cu⋯Cu Distances (Å) and Calculated  $J$  Values at Different Temperatures

	temperature			
	293 K	100 K	40 K	10 K
space group	$I2/a$	$I2/a$	$I2/a$	$P\bar{1}$
Cu–N1(bpym1)	2.118(2)	2.050(2)	2.052(3)	2.029(3)
Cu–N2(bpym1)	2.185(2)	2.306(2)	2.301(3)	2.275(4)
Cu–N5/N6(bpym2)				2.310(4)/2.071(3)
Cu–N3/N4(tnnoet)	2.049(2)	1.989(2)	1.993(3)	1.998(4)/1.988(3)
⟨Cu–N⟩	2.117	2.115	2.115	2.112
Cu–bpym–Cu	5.741(1)	5.785(1)	5.779(1)	5.731(1)/5.827(1)
$J_{\text{calc}}$ (cm <sup>-1</sup> )	+3.83	+1.31	+1.66	−0.50/+2.43

One of the CN groups and a water molecule are statistically disordered over two sites. The most interesting structural feature of **1** at room temperature concerns the geometry of the CuN<sub>6</sub> coordination sphere, which significantly deviates from the usual elongated octahedral distorted geometry [ $D_{4h}$  symmetry due to the Jahn–Teller (JT) distortion] observed for most Cu<sup>II</sup> complexes (Table 1). In order to determine the thermal evolution of this unusual geometry, we have solved the crystal structure at different temperatures between 293 and 100 K (see Table S1 in the Supporting Information).<sup>8</sup> These measurements indicate the presence of a gradual thermochromism when a single crystal of **1** is cooled from room temperature to 100 K (see the inset in Figure 2 and Figure S1 in the Supporting Information). Preliminary UV–vis spectroscopic measurements confirm, as expected,

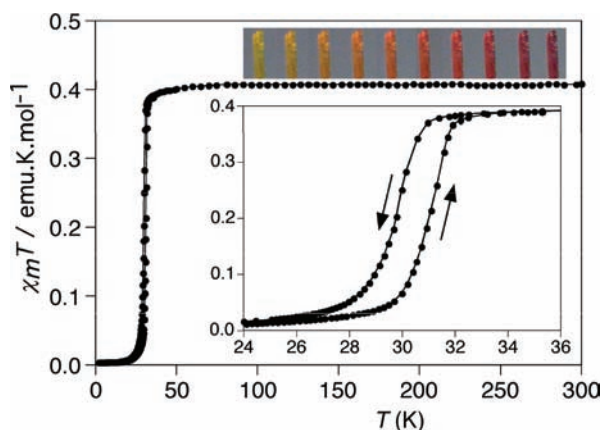


**Figure 2.** Thermal variation of the  $\chi_m T$  product for compound **1**. Insets show the hysteresis in the magnetic transition around 30 K and the progressive reversible thermochromism.

the presence of such a thermochromic transition. This thermochromism is due to a dynamic pseudo-JT effect that is progressively frozen as the temperature is lowered to 100 K. At that temperature, and down to 40 K, the static distortion of the Cu<sup>II</sup> environment points to the Cu–N2 bond direction as the octahedron elongation axis. The JT fluxionality is nicely evidenced at room temperature by inspection of the thermal ellipsoids (Figure S2 in the Supporting Information) and by the temperature dependence of the apparent Cu–N bond distances (Figure S1 in the Supporting Information), typical for such a dynamic JT effect.<sup>9</sup> This behavior slightly changes the average ligand field, leading to a gradual color change of the crystals from dark red at room temperature to yellow at 100 K.

The product of magnetic susceptibility times temperature per Cu<sup>II</sup> ion ( $\chi_m T$ ) remains constant at 0.41 emu·K·mol<sup>-1</sup> from room temperature down to ca. 30 K, indicating that compound **1** is essentially paramagnetic above 30 K [the calculated  $J$  values using density functional theory (DFT) indicate the presence of a weak ferromagnetic coupling; Table 1]. Below 30 K,  $\chi_m T$  shows an unexpected reversible sharp drop from ca. 0.4 to ca. 0.0 emu·K·mol<sup>-1</sup> (Figures 2 and S3 in the Supporting Information). On an increase of the temperature, a slight hysteresis of ca. 2.0 K was detected (see the inset in Figure 2). These temperatures are independent of the applied magnetic field and of the number of cycles.

To understand the origin of the magnetic transition in **1**, we have determined the crystal structure just above (40 K) and below (10 K) the magnetic transition.<sup>8</sup> At 40 K, the structure of **1** is the same as that at 100 K, whereas at 10 K (well below the transition temperature), a lowering of the symmetry from the monoclinic  $I2/a$  space group to the triclinic  $P\bar{1}$  space group is observed. As a consequence of this symmetry breaking, the unit cell volume at 10 K is reduced to a primitive one. Consequently, the Cu point symmetry decreases from 2 to 1 and the centrosymmetric bpym ligands are not crystallographi-

(8) Crystallographic studies of complex **1** were performed in the temperature range 293–10 K. Crystal data for **1** at 293 K: C<sub>26</sub>H<sub>18</sub>CuN<sub>12</sub>O<sub>3</sub>,  $M_w = 610.06$  g·mol<sup>-1</sup>, monoclinic, space group  $I2/a$ ,  $a = 10.0792(6)$  Å,  $b = 11.9676(5)$  Å,  $c = 24.9148(12)$  Å,  $\beta = 89.467(4)^\circ$ ,  $V = 3005.2(3)$  Å<sup>3</sup>,  $Z = 4$ ,  $\rho_{\text{calcd}} = 1.348$  g·cm<sup>-3</sup>,  $F_{000} = 1244$ , 7659 collected reflections, 2163 unique ( $R_{\text{int}} = 0.0242$ ), final GOF = 1.066 (all data),  $R1 = 0.0374$ ,  $wR2 = 0.0949$ ,  $R$  indices based on 1958 reflections with  $I > 2\sigma(I)$ , 245 parameters. Crystal data at 100 K:  $a = 10.1105(5)$  Å,  $b = 11.8149(6)$  Å,  $c = 24.9214(12)$  Å,  $\beta = 91.839(4)^\circ$ ,  $V = 2975.4(3)$  Å<sup>3</sup>,  $Z = 4$ ,  $\rho_{\text{calcd}} = 1.362$  g·cm<sup>-3</sup>,  $F_{000} = 1244$ , 7620 collected reflections, 2497 unique ( $R_{\text{int}} = 0.0305$ ), final GOF = 1.081 (all data),  $R1 = 0.0351$ ,  $wR2 = 0.0874$ ,  $R$  indices based on 2223 reflections with  $I > 2\sigma(I)$ , 225 parameters. Crystal data at 40 K:  $a = 10.1192(16)$  Å,  $b = 11.7954(12)$  Å,  $c = 24.897(2)$  Å,  $\beta = 91.787(11)^\circ$ ,  $V = 2970.2(6)$  Å<sup>3</sup>,  $Z = 4$ ,  $\rho_{\text{calcd}} = 1.364$  g·cm<sup>-3</sup>,  $F_{000} = 1244$ , 12 181 collected reflections, 4035 unique ( $R_{\text{int}} = 0.0242$ ), final GOF = 1.074 (all data),  $R1 = 0.0661$ ,  $wR2 = 0.1516$ ,  $R$  indices based on 2842 reflections with  $I > 2\sigma(I)$ , 245 parameters. Crystal data at 10 K: triclinic, space group  $P\bar{1}$ ,  $a = 10.1400(4)$  Å,  $b = 11.8050(7)$  Å,  $c = 14.5310(5)$  Å,  $\alpha = 66.091(4)^\circ$ ,  $\beta = 70.285(4)^\circ$ ,  $\gamma = 87.905(5)^\circ$ ,  $V = 1486.76(12)$  Å<sup>3</sup>,  $Z = 2$ ,  $\rho_{\text{calcd}} = 1.363$  g·cm<sup>-3</sup>,  $F_{000} = 622$ , 10 705 collected reflections, 5761 unique ( $R_{\text{int}} = 0.0246$ ), final GOF = 1.078 (all data),  $R1 = 0.0714$ ,  $wR2 = 0.1870$ ,  $R$  indices based on 4892 reflections with  $I > 2\sigma(I)$ , 364 parameters.

(9) (a) Bebandorf, J.; Burgi, H.-B.; Gamp, E.; Hitchman, M. A.; Murphy, A.; Reinen, D.; Riley, M. J.; Stratemeier, H. *Inorg. Chem.* **1996**, *35*, 7419. (b) Falvello, L. R. *J. Chem. Soc., Dalton Trans.* **1997**, 4463. (c) Halcrow, M. A. *Dalton Trans.* **2003**, 4375.

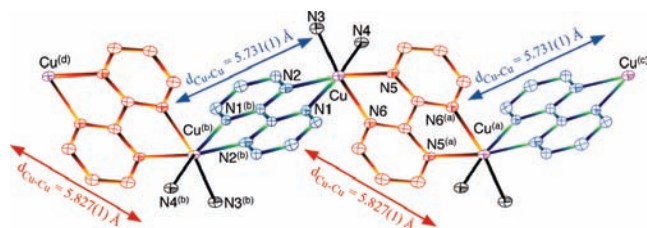


**Figure 3.** Dimerized chain structure of compound **1** at 10 K.

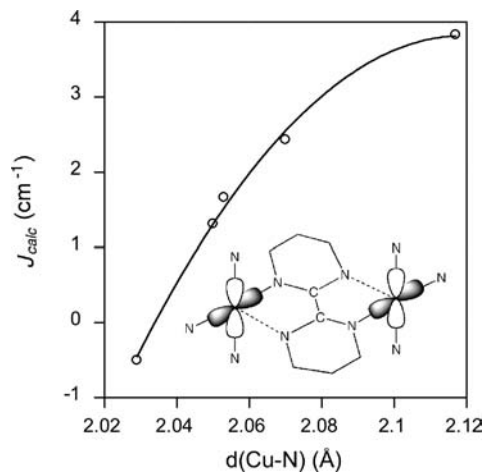


**Figure 4.** Dependence of the calculated  $J$  value with the short Cu–N1 bond. The inset shows the magnetic orbitals in the Cu<sup>II</sup> centers.

cally equivalent any more. This leads to a dimerization of the polymeric zigzag chain with two alternating Cu<sup>•••</sup>Cu distances (Table 1 and Figure 3) and to a complete ordering of the CN and H<sub>2</sub>O groups.

In order to explain the magnetic behavior and its correlation with the structural changes, we have carried out electronic structure calculations using DFT methods for an estimation of the exchange-coupling constants at different temperatures using dinuclear models and keeping the bpym and tcnocet ligands.<sup>10</sup> Thus, from the crystal data, we have estimated the coupling constants ( $J$ ) at different temperatures using dinuclear models. These  $J$  values show a weak ferromagnetic coupling for the regular chain (as expected from the perpendicular orientation of the magnetic orbitals) that decreases when the temperature is lowered (Table 1 and Figure 4).

The bpym ligand is known for its ability to transmit antiferromagnetic coupling when acting as a bis-bidentate ligand connecting paramagnetic centers separated by more than 5.5 Å.<sup>5,11</sup> As shown in Table 1, when the sample is cooled from room temperature to 100 K, the two longest Cu–N2 distances increase while the two shortest Cu–N1

ones decrease, remaining constant from 100 K down to the transition temperature. Such an unusual thermal evolution leads to a decrease in the coupling constant ( $J$ ) along the chain (Table 1) and, therefore, to magnetic isolation of the Cu<sup>II</sup> ions as the temperature decreases, in agreement with the paramagnetic behavior observed in **1** down to 30 K (Figure 2). Below the magnetic transition, the dimerized chain presents two alternating bpym bridges: a short one and a long one (bpym1 and bpym2, respectively; see Table 1 and Figure 3). The bpym2 bridge transmits a ferromagnetic coupling (although weak), whereas the bpym1 bridge mediates a weak antiferromagnetic coupling due to the shortening of the Cu–N1 distance, which is the key factor controlling the nature and strength of the exchange (Figure 4). In good agreement with the observed sharp drop of the  $\chi_m T$  product, this alternation of ferro- and antiferromagnetic interactions along the chain leads to an  $S = 0$  spin ground state.

In summary, we have prepared and characterized a Cu<sup>II</sup> coordination polymer exhibiting two different unusual transitions: an unprecedented reversible structural transition leading to an abrupt magnetic transition at 30 K with a hysteresis of ca. 2 K and a reversible progressive thermochromic transition at high temperatures. The thermochromism is due to a dynamic pseudo-JT effect that is progressively frozen as the temperature is lowered to 100 K. The crystal structure determination at 10 K shows a dimerized chain structure of **1** clearly different from the regular chain observed in the temperature range 40–293 K. Although a similar dimerization is also observed in the SP transitions, the title compound cannot be considered as such because the magnetic coupling before the transition is not antiferromagnetic and, therefore, the driving force in this transition is not the decrease in energy due to the antiferromagnetic coupling, as is to be expected in SP transitions. It seems that in the title compound the magnetic transition is produced by the structural changes driven by the JT thermal evolution operating in the Cu<sup>II</sup> ions. This assumption is supported by the complete ordering of the CN and H<sub>2</sub>O groups after the magnetic transition.

**Acknowledgment.** The authors acknowledge the CNRS, Brest and Nancy Universities, the Ministère de la Recherche (PPF “Cristallographie et Photocristallographie à haute résolution”), the European Union (COST Action D35 and MAGMANet network of excellence), and the Spanish Ministerio de Educación y Ciencia (Projects CTQ2005-08123-C02-02/BQU, MAT2007-61584, and CSD 2007-00010 Consolider-Ingenio in Molecular Nanoscience) for financial support.

**Supporting Information Available:** Crystallographic data (CIF) at different temperatures, thermal evolution of the Cu<sup>II</sup> coordination sphere, and a  $\chi_m^{-1}$  vs  $T$  plot. This material is available free of charge via the Internet at <http://pubs.acs.org>.

IC802292S

(10) (a) Ruiz, E.; Alemany, P.; Alvarez, S.; Cano, J. *J. Am. Chem. Soc.* **1997**, *119*, 1297. (b) Ruiz, E.; Cano, J.; Alvarez, S.; Alemany, P. *J. Comput. Chem.* **1999**, *20*, 1391.

(11) (a) De Munno, G.; Poerio, T.; Julve, M.; Lloret, F.; Faus, J.; Caneschi, A. *J. Chem. Soc., Dalton Trans.* **1998**, 1679. (b) Castro, I.; Sletten, J.; Glaerum, L. K.; Cano, J.; Lloret, F.; Faus, J.; Julve, M. *J. Chem. Soc., Dalton Trans.* **1995**, 3207. (c) De Munno, G.; Julve, M.; Lloret, F.; Cano, J.; Caneschi, A. *Inorg. Chem.* **1995**, *34*, 2048. (d) De Munno, G.; Julve, M.; Verdaguer, M.; Bruno, G. *Inorg. Chem.* **1993**, *32*, 2215.